Title Page

CYP3A4 and *CYP3A5* expression is regulated by C*YP3A4*1G* in CRISPR/Cas9 edited HepG2 cells

Weihong Yang, Huan Zhao, Yaojie Dou, Pei Wang, Qi Chang, Xiaomeng Qiao, Xiaofei Wang, Chen Xu, Zhe Zhang, Lirong Zhang

Department of Forensic Medicine, School of Basic Medical Sciences, Zhengzhou University, Zhengzhou, 450001, China (W.Y, H.Z, Y.D, X.Q, C.X)

Department of Pharmacology, School of Basic Medical Sciences, Zhengzhou University, Zhengzhou, 450001, China (P.W, Q.C, X.W, L.Z)

Department of Gastroenterology, the Second Affiliated Hospital of Zhengzhou University, Zhengzhou, 450014, China (Z.Z)

Running Title: rs2242480 regulates the expression of *CYP3A4* and *CYP3A5*

Corresponding Author:

Dr. Lirong Zhang, Department of Pharmacology, School of Basic Medical Sciences, Zhengzhou University, Zhengzhou, Henan, China. Phone: +86 371-66658807; E-mail: zhanglirongzzu@126.com.

Number of text pages:36

Number of tables: 0

Number of figures: 6

Number of references: 38

Number of words in abstract: 196

Number of words in introduction: 726

Number of words in discussion: 1356

Abbreviations: CRISPR/Cas9, clustered regularly interspaced short palindromic repeats/CRISPR-associated protein 9; *CYP3A4,* cytochrome P450 *3A4*; DMSO, dimethyl sulfoxide; EGFP, enhanced green fluorescent protein; ER6, everted repeat sequence separated by 6 bp; HDR, homology-directed repair; PAM, protospacer adjacent motif; PCR, polymerase chain reaction; px330, PX330a-42230; PXR, pregnane X receptor; RIF, rifampicin; sgRNA, single guide RNA; SNP, single nucleotide polymorphism.

DMD Fast Forward. Published on January 9, 2023 as DOI: 10.1124/dmd.122.001111
This article has not been copyedited and formatted. The final version may differ from this version.

Abstract

Functional *CYP3A4*1G* (G>A, rs2242480) in cytochrome P450 *3A4* (*CYP3A4*) regulates the drug-metabolizing enzyme *CYP3A4* expression. The objective of this study was to investigate whether *CYP3A4*1G* regulates both basal and rifampicin (RIF)-induced expression and enzyme activity of *CYP3A4* and *CYP3A5* in gene-edited human HepG2 cells**.** *CYP3A4*1G* GG and AA genotype HepG2 cells were established using the clustered regularly interspaced short palindromic repeats/CRISPR-associated protein 9 (CRISPR/Cas9) single nucleotide polymorphism (SNP) technology and homology-directed repair (HDR) in the *CYP3A4*1G* GA HepG2 cell line. In *CYP3A4*1G* GG, GA, and AA HepG2 cells, *CYP3A4*1G* regulated expression of *CYP3A4* and *CYP3A5* mRNA and protein in an allele-dependent manner. Of note, significantly decreased expression level of *CYP3A4* and *CYP3A5* was observed in *CYP3A4*1G* AA HepG2 cells. Moreover, the results after RIF treatment showed that *CYP3A4*1G* decreased the induction level of *CYP3A4* and *CYP3A5* mRNA expression in *CYP3A4*1G* AA HepG2 cells. At the same time, *CYP3A4*1G* decreased CYP3A4 enzyme activity and tacrolimus metabolism especially in *CYP3A4*1G* GA HepG2 cells. In summary, we successfully constructed *CYP3A4*1G* GG and AA homozygous HepG2 cell models and found that *CYP3A4*1G* regulates both basal and RIF-induced expression and enzyme activity of *CYP3A4* and *CYP3A5* in CRISPR/Cas9 *CYP3A4*1G* HepG2 cells.

Significance Statement

*CYP3A4*1G* regulates both basal and RIF-induced expression and enzyme activity of *CYP3A4* and *CYP3A5*. This study successfully established *CYP3A4*1G* (G>A, rs2242480), GG, and AA HepG2 cell models using CRISPR/Cas9; thus providing a powerful tool for studying the mechanism by which *CYP3A4*1G* regulates the basal and RIF-induced expression of *CYP3A4* and *CYP3A5*.

Introduction

In human adult livers, CYP3A, and its major components, CYP3A4 and CYP3A5, plays a crucial role in clinical drug metabolism, by metabolizing more than 60% of clinical prescription drugs. Genetic variation in *CYP3A4*, such as the single nucleotide polymorphism (SNP) *CYP3A4*22* (rs35599367, G>A) in intron 6, which affects its transcript splicing, decreases *CYP3A4* expression (Wang and Sadee, 2016), resulting in improved pharmacokinetics and clinically effective therapy (Wang *et al*., 2011 Mulder *et al*., 2021). The intronic genetic variation in *CYP3A5*, *CYP3A5*3* (rs776746, A>G), leads to decreased normal *CYP3A5* expression through alternative splicing (Kuehl *et al*., 2001) and is associated with tacrolimus dosage and pharmacokinetics (Dorr *et al*., 2017; Tang *et al*., 2019). Recently these two SNPs have become biomarkers for clinical individualized medications. Therefore, elucidating the mechanisms of individual differences in CYP3A enzyme activity from the perspective of intron SNP variation can provide new ideas for the implementation of precise and individualized treatments. Interestingly, another important *CYP3A4* variation, *CYP3A4*1G* (rs2242480, G>A) (Fig.1), is an intronic SNP enhancer (He *et al*., 2011; Yang *et al*., 2015) that is suspected to be a vital SNP in regulation of *CYP3A4* expression and enzyme activity.

*CYP3A4*1G* is associated with the metabolism of numerous drugs (Gao *et al*., 2008; Zhang *et al*., 2010; Yuan *et al*., 2011; Dong *et al*., 2012; Ren *et al*., 2015; Yuan *et al*., 2015; Zhang *et al*., 2017; Lv *et al*., 2018; Zhang *et al*., 2018). CYP3A5 and CYP3A4 have highly substrate similarity, and CYP3A5 can metabolize most of

substrates metabolized by CYP3A4. *CYP3A5**3, which causes protein truncation, results in the absence of normal *CYP3A5* expression, while *CYP3A5**1 is related to normal CYP3A5 expression. Although *CYP3A5**3 linkage with *CYP3A4*1G* might interfere with the metabolism of drugs metabolized by CYP3A4, the relation between *CYP3A4*1G* and tacrolimus in *CYP3A5* expressers, or atorvastatin in *CYP3A5* non-expressers, were further confirmed (Miura *et al*., 2011; He *et al*., 2014; Liu *et al*., 2017). Moreover, the allele frequency of *CYP3A4*1G* highly differs between ethnic lines, and its global allele frequency is about 0.15 (ranging between about 0.09 and 0.86 among 11 populations). Nine out of the eleven populations have allele frequencies over 0.28 (https://www.ncbi.nlm.nih.gov/snp/rs2242480#frequency_tab). Using luciferase enhancer reporter assays, we previous showed that *CYP3A4*1G*, in the full-length of *CYP3A4* intron 10, as an enhancer, regulates the expression of *CYP3A4* (Yang *et al*., 2015). However, since suitable *CYP3A4*1G* cell models are unavailable due to *CYP3A4*1G* strong linkage with *CYP3A5*3* (Fig.1), the mechanism is not clear. It is still unclear whether the enhancer, *CYP3A4*1G*, regulates *CYP3A4* expression and enzyme activity in the native chromatin context of *CYP3A4*1G* in living cells of different genotypes, as reporter gene assays inherently disconnect regulatory elements from their target genes and may not reflect in-vivo activity (Bu and Gelman, 2007; Kato *et al*., 2007; Wang *et al*., 2008). Now, precision SNP clustered regularly interspaced short palindromic repeats/CRISPR-associated protein 9 (CRISPR/Cas9) mediated homology-directed repair (HDR) technology is available (Hegde *et al*., 2021). Thus, the establishment of a human *CYP3A4*1G* liver

cell line by CRISPR/Cas9 technology may lay the foundation to explore the relationship between the intronic SNP variation of *CYP3A4* gene, its regulatory mechanism, and drug metabolism.

HepG2 cells, a hepatoblastoma cell line derived from human liver tissue of a 15-year-old white male from the Caucasian region (López-Terrada *et al*., 2009), are commonly used for *in vitro* drug metabolism studies. The genotypes of *CYP3A4*1G*, *CYP3A5*3*, and *CYP3A4*22* in HepG2 cells are GA, AG, and CC, respectively (Zhao YL, 2016). Therefore, HepG2 cells are suitable for being edited to *CYP3A4*1G* GG and AA HepG2 cell strains. In HepG2 cells, as *CYP3A5*3* is highly linked with *CYP3A4*1G*, we speculated *CYP3A4*1G* was related to *CYP3A5* expression and enzyme activity. Rifampicin (RIF), as a strong inducer, can increase *CYP3A4* expression through the pregnane X receptor (PXR). However, it is not clear whether RIF may induce the expression of *CYP3A* in gene-edited *CYP3A4*1G*, GG, and AA HepG2 cells.

In this study, we established *CYP3A4*1G*, GG, and AA HepG2 cell strains successfully using CRISPR/Cas9 technology. We further verified that *CYP3A4*1G* regulated both basal and RIF-induced expression, and the metabolism of *CYP3A4* and *CYP3A5* in *CYP3A4*1G* HepG2 cells. These findings will enrich the basic theory that *CYP3A4* intron enhancer SNP regulates the expression and enzyme activity of *CYP3A4* and *CYP3A5* and provide a new idea for accounting for the variability of CYP3A activity and clinical precision medicine.

Materials and Methods

Cell lines

HepG2 and HEK293T cells were obtained from Stem Cell Bank, Chinese Academy of Sciences (Shanghai, China) and cultured in a high-sugar DMEM medium supplemented with 10% fetal bovine serum, 100 U/mL penicillin, and 100 μ g/mL streptomycin at 37℃ with 5% CO_2.

Establishment of *CYP3A4*1G* GG and AA HepG2 cells by CRISPR/Cas9

Construction and identification of px330 and pmCherry enhanced green fluorescent protein (EGFP) reporter recombination plasmids

According to human *CYP3A* GenBank AF280107.1 from the National Center for Biotechnology Information, single guide RNA (sgRNA), pmCherry EGFP reporter sequences and HDR template containing *CYP3A4*1G* G or A allele were designed by software ZiFiT and Vector NTI 11.5.1 respectively. PX330a-42230 (px330) and pmCherry EGFP reporter vectors were kindly donated by Professor Yaohe Wang in Sino-British Research Centre for Molecular Oncology, National Centre for International Research in Cell and Gene Therapy, Academy of Medical Sciences, Zhengzhou University. The above sgRNA and pmCherry EGFP reporter sequences (Fig.2, Supplemental Table 1) were synthesized (Shanghai Shenggong Co., Ltd, China) and inserted to px330 and pmCherry EGFP reporter vectors and verified by enzyme digestion and sequencing (Shanghai Shenggong Co., Ltd).

*Establishment of CYP3A4*1G GG and AA HepG2 cell strains*

In order to achieve *CYP3A4*1G* wildtype (GG) and mutant type (AA),

homozygous HepG2 cells, CRISPR/Cas9 mediated HDR templates (Supplemental Table 1) were synthesized (Jinsirui Biotechnology Co., Ltd., Nanjing, China). The above px330-sgRNA, pmCherry EGFP reporter recombinant vectors along with the corresponding HDR templates were co-transfected into *CYP3A4*1G* GA HepG2 cells using Lipofectamine 2000 (Thermo Fisher Scientific, Carlsbad, CA, USA) following the manufacturer's instructions. Higher efficiency px330-sgRNA (1.5 μg), pmCherry EGFP-reporter (1.5 μg) and corresponding HDR templates (10 μM, 5 μL) were used according to the proportion 1:3 of DNA (μg): Lipofectamine 2000 (μL). Forty-eight hours post transfection in 6 well plates, the objective HepG2 cells were collected and sorted using the BD FACSCanto flow cytometry instruments from BD Biosciences (San Jose, CA, USA) and cultured in monoclonal cell way into 96 well plates. Finally, their genomic DNA was extracted and polymerase chain reaction (PCR) amplified. The PCR products were sequenced to screen *CYP3A4*1G* GG and AA monoclonal HepG2 cell strains. Primers used are shown (Supplemental Table 2).

Validation of off-target objective HepG2 cell strains

In order to ensure there were potential off-target sites of the sgRNA-2W and sgRNA-3M in screened *CYP3A4*1G* GG and AA HepG2 cells, the potential off-target gene sequence and its location on chromosome (Supplemental Table 3) were predicted. Primers for several predicted top off-target locations (Supplemental Table 3) were designed online (*https://zlab.bio/guide-design-resources*), and off-target situations in above HepG2 cells were evaluated by sequencing of PCR products.

Examination of basal expression of *CYP3A4* and *CYP3A5* mRNA and protein

mRNA analysis

Total RNA was extracted from *CYP3A4*1G* GG, GA, and AA HepG2 cells using TRizol Reagent (TIANGEN, Bei Jing, China) according to the manufacturer's instructions. cDNA was reverse transcribed from total RNA, and 5 ng cDNA was amplified using an iQ5 Real-Time PCR Detection System with SYBR Green Master Mix from Thermo Fisher Scientific. Primers used are shown in Supplemental Table 2. The relative expression of *CYP3A4, CYP3A5* and *PXR* was calculated by $2^{-\triangle\triangle Ct}$ method, and normalized to *GAPDH*.

Western blot Analysis

Total proteins of the above *CYP3A4*1G* GG, GA, and AA HepG2 cells were prepared using RIPA buffer. Protein concentrations were determined by BCA Protein Assay. Protein samples were separated by 12% SDS polyacrylamide gel electrophoresis and transferred to polyvinylidene difluoride membranes. The membranes were blocked with 5% non-fat dried milk in 1×tris buffered saline, 0.1 % Tween-20 and incubated overnight with primary antibodies for CYP3A4 or CYP3A5 (Abcam) at 1/1000 dilution. The next day, the membranes were incubated in horseradish peroxidase-labeled secondary antibodies and visualized with an enhanced chemiluminescence method. Anti-GAPDH (Abcam) at 1/5000 was used as a loading control.

Detection of *CYP3A4* and *CYP3A5* induction expression

*CYP3A4*1G* GG, GA, and AA HepG2 cells cultured in 12 well plates were treated with 10 μM RIF (Sigma-Aldrich, St. Louis, MO) for 48 h prior to harvesting,

CYP3A4, CYP3A5 and *PXR* mRNA expression levels were examined by quantitative real-time polymerase chain reaction.

CYP3A4 enzyme activity and tacrolimus metabolism study

P450-Glo™ CYP3A4 assay

*CYP3A4*1G* GG, GA and AA HepG2 cells were washed with phosphate buffered saline and luminescence was measured using the P450-Glo™ CYP3A4 assay kit and Luciferin-IPA (Promega, Cat # V9001) with a plate reader as previous described (Pande *et al*., 2020).

Tacrolimus Metabolism Assays

*CYP3A4*1G* GG, GA, and AA HepG2 cells were treated with tacrolimus and incubated for 24 h. Tacrolimus from Dalian Meilun Biotechnology Co., Ltd (Shanghai, China) was diluted in methanol (1 mg/mL) so that tacrolimus final concentration in cell culture medium was 50 ng/mL. Media were collected and assayed for tacrolimus by ultra-high-performance liquid chromatography-mass spectrometry system according to previously described methods with minor modifications (Dorr *et al*., 2017; Liu *et al*., 2020; Shi *et al*., 2022). Collected media were centrifuged, and 40 μL supernatant with 160 μL glacial acetonitrile were vortexed for 30 s and placed on ice for 20 min before being centrifuged again. The supernatants were dried and resuspended in 320 μL methanol and mixed with 40 μL of internal standard (ascomycin, 2000 ng/mL, dissolved in methanol) from Dalian Meilun Biotechnology Co., Ltd (Shanghai, China). After vortexing and centrifugation at 14000×g for 30 min at 4 ℃, the supernatants were filtered with a membrane and placed in a liquid

injection flask. The residual amount of tacrolimus in the sample was determined using ultra-high-performance liquid chromatography-mass spectrometry including Shimadzu LC-30A system and 6500 QTRAP triple quadrupole mass spectrometer equipped with an ESI source) (ABSCIEX, USA). The mobile phase A was ammonium acetate aqueous solution, and mobile phase B was methanol. Loading volume was 3 μL. An Atlantis T3 column (2.1 mm × 100 mm, 3μm) was used, and the column temperature was 40 ℃. The transitions (precursor to product) monitored are m/z 821.7 to 768.5 for tacrolimus and m/z 809.7 to 729.6 for the internal standard, respectively. Ionization was performed in positive ion mode with a capillary voltage of 5.5 kV, a cone voltage of 61/74 (tacrolimus/internal standard), an ion source temperature of 550 ℃, and a collision gas pressure of 27.8/21 V (tacrolimus/internal standard).

Statistical analysis

Statistical analysis was performed using Statistical Product and Service Solutions 21.0 software (IBM, Armonk, NY, USA). All comparisons were conducted using one-way or two-way ANOVA with Bonferroni *post hoc* test. Data were shown as mean ± S.D. $P < 0.05$ was considered statistically significant.

Results

Establishment of *CYP3A4*1G* GG and AA HepG2 cells by CRISPR/Cas9 technology

Identification of px330 and pmCherry EGFP reporter recombination plasmids

Sequencing results verified the sequences and directions of positive recombination plasmids, px330-sgRNA and pmCherry EGFP reporter with inserted target fragment sequences (Supplemental Fig.1A, B), correct.

*Identification of gene-edited CYP3A4*1G GG and AA HepG2 cells*

The efficiency of the sgRNA expression vector was screened in HEK293T cells (Supplemental Fig.1C). In order to construct *CYP3A4*1G*, GG, and AA HepG2 cells, objective px330-sgRNA, pmCherry EGFP reporter recombinant vectors and the corresponding homologous recombination repair templates were co-transfected into *CYP3A4*1G* GA HepG2 cells. Monoclonal cells of the objective HepG2 cells were sorted and cultured. Identification of gene-edited *CYP3A4*1G* GG and AA HepG2 cells was performed by genomic DNA extraction, PCR amplification, and sequencing. Results of sequencing indicated that the genotypes of objective *CYP3A4*1G* GG and AA HepG2 cell strains were both homozygous compared with *CYP3A4*1G* GA HepG2 cells (Fig.3). In *CYP3A4*1G* GG HepG2 cells the sequencing alignment (Supplemental Fig.2A) unexpectedly revealed a deletion of two continuous bases (GA) at the 9^{th} and 10^{th} sites downstream of the *CYP3A4*1G* G allele in *CYP3A4* intron 10. For *CYP3A4*1G* AA HepG2 cells, there was one base deletion in 11^{th} base (A) downstream of the *CYP3A4*1G* A allele. Above all, the *CYP3A4*1G* point mutation

was correctly edited, and the *CYP3A4*1G* wildtype and mutant homozygote HepG2 cell strains were successfully constructed.

Off-target effects validation of monoclonal cells

Genomic DNA of *CYP3A4*1G* GG, GA, and AA HepG2 cells was subjected to PCR and sequencing using off-target primers. Comparing the sequencing results with the predicted off-target sequences showed 8 sequences without off-target (Supplemental Fig.3A, 3B), and 2 near sequences, 3M-2 and 2W-1, off-target in these 10 sequences. The off-target sequence in *CYP3A4*1G* GG HepG2 was the second sequence, 3M-2 GAGTGGA**CA**GTACATGGAGAA on chr7: -99710713 predicted by sgRNA-3M, where there was a base A insertion, highlighted by underline (Supplemental Fig.2B). In *CYP3A4*1G* AA HepG2, the off-target sequence very near 3M-2 was the first sequence, 2W-1 GGA**CA**GTACATGGAGAAGGA on chr7: -99710709 predicted by sgRNA-2W, where there was a 14 bp deletion, shown by underlined sequence, on chr7 (99710723-99710710) *CYP3A7* intron 10, as well as four SNP homozygous mutations in *CYP3A7* exon 10 (Supplemental Fig.2B). The genotypes of these SNPs were rs754782383 (T>C) CC 90th, rs777212283 (C>T) new mutation C>G GG 127th, rs1336177699 (T>G) new mutation T>C CC 133th, and rs756922005 (T>C) CC 145th in the exon 10 of *CYP3A7*. *CYP3A4*1G* GG and AA HepG2 were used for further study.

CYP3A4*1G* regulates basal expression of *CYP3A4* and *CYP3A5

Basal expression levels of *CYP3A4* and *CYP3A5* mRNA and protein in *CYP3A4*1G* GG, GA and AA HepG2 cells were examined by quantitative real-time

polymerase chain reaction and western blot. *CYP3A4* mRNA expression levels decreased in *CYP3A4*1G* AA HepG2 cells compared with *CYP3A4*1G* GG and GA HepG2 cells (both $P < 0.01$), and *CYP3A4* mRNA expression in *CYP3A4*1G* GA HepG2 cells was lower than that in *CYP3A4*1G* GG HepG2 cells ($P < 0.01$) (Fig. 4A). Moreover, CYP3A4 protein expression level also decreased in *CYP3A4*1G* AA HepG2 cells compared with *CYP3A4*1G* GG ($P < 0.01$) and GA HepG2 cells, despite the fact that there was no significant difference between *CYP3A4*1G* AA and GA HepG2 cells (Fig.4B). These results indicate that *CYP3A4*1G* regulates the mRNA and protein expression levels of *CYP3A4* in an allele-dependent manner. As *CYP3A5*3* showed linkage with *CYP3A4*1G*, *CYP3A5* mRNA and protein expression levels were also examined. Similarly, *CYP3A4*1G* also regulated *CYP3A5* mRNA and protein expression in an allele dependent-manner (Fig.4C-4D). *CYP3A5* mRNA expression level in *CYP3A4*1G* AA HepG2 cells was lower than that in *CYP3A4*1G* GG HepG2 cells ($P < 0.01$), and there was a significant difference for *CYP3A5* mRNA expression level between *CYP3A4*1G* GA and GG HepG2 cells ($P < 0.05$) (Fig.4C). The protein expression levels of CYP3A5 were also lower in *CYP3A4*1G* AA HepG2 cells than that in *CYP3A4*1G* GG and GA HepG2 cells ($P < 0.01$ or $P < 0.05$), and there was also a significant difference for CYP3A5 protein expression levels between *CYP3A4*1G* GA and GG HepG2 cells ($P < 0.05$) (Fig.4D). In summary, *CYP3A4*1G* regulates basal expression of *CYP3A4* and *CYP3A5* at both mRNA and protein levels.

CYP3A4*1G decreases RIF-induced expression of _CYP3A4_ and _CYP3A5_

RIF, a strong inducer of CYP3A4 enzyme, can induce *CYP3A4* expression by PXR; therefore, we investigated the impacts of *CYP3A4*1G* on the RIF-induced *CYP3A4* and *PXR* expression in different *CYP3A4*1G* HepG2 cells. As shown in Fig. 5A, RIF could induce the *CYP3A4* mRNA expression levels in *CYP3A4*1G* GG, GA, and AA HepG2 cells, as compared to the control group ($P < 0.01$ or $P < 0.05$). However, diminished induction levels of *CYP3A4* by RIF were observed in the *CYP3A4*1G* AA and GA HepG2 cells as compared to the *CYP3A4*1G* GG HepG2 cells. RIF increased *CYP3A4* mRNA expression in the above three different *CYP3A4*1G* genotype HepG2 cells in an allele-dependent manner as compared to the dimethyl sulfoxide (DMSO) alone control groups, with the induction of *CYP3A4*1G* AA and GG HepG2 cells being the weakest and the strongest (over 6 folds *CYP3A4* mRNA expression), respectively. The roles of induction of RIF in *CYP3A4*1G* GA HepG2 cells was between them. These results suggest that RIF induces *CYP3A4* mRNA expression in *CYP3A4*1G* allele-dependent manner.

*CYP3A4*1G* also affected *CYP3A5* mRNA expression, therefore we analyzed whether RIF could also induce *CYP3A5* expression. Similar to *CYP3A4* induction by RIF, *CYP3A4*1G* decreased *CYP3A5* mRNA expression. Comparing the same *CYP3A4*1G* genotype HepG2 cells between RIF and DMSO groups, *CYP3A5* mRNA expression was also all increased after RIF treatment; however, the extent of induction of RIF in *CYP3A4*1G* AA HepG2 cells was much lower than that in *CYP3A4*1G* GG and GA HepG2 cells. There was significant difference in *CYP3A4*1G* GG or GA HepG2 cells after being induced ($P < 0.01$ or $P < 0.05$). RIF induction in *CYP3A4*1G*

GG HepG2 cells was over 6 folds the *CYP3A5* mRNA expression of the same genotype HepG2 cells in the DMSO group (Fig.5B). These results indicate that RIF also induces *CYP3A5* mRNA expression in a *CYP3A4*1G* allele-dependent manner, and its induction level in *CYP3A4*1G* AA HepG2 cells is much lower than that in *CYP3A4*1G* GG HepG2 cells.

Since RIF-induced *CYP3A4* by PXR, PXR mRNA expression levels in different *CYP3A4*1G* genotype HepG2 cells were also determined. Comparing *PXR* expression between DMSO and RIF group, we found that *PXR* mRNA expression level in *CYP3A4*1G* GG HepG2 cells was much higher in RIF group than that in DMSO group ($P < 0.05$); however, *PXR* mRNA expression levels in the other genotype HepG2 cells were not significantly increased (Fig.5C). Particularly, diminished basal and RIF-induced mRNA expression levels of *PXR* were observed in the *CYP3A4*1G* AA (both $P < 0.05$) and GA HepG2 cells (both $P < 0.05$) as compared to the *CYP3A4*1G* GG HepG2 cells. These results reveal that *CYP3A4*1G* decreases basal and RIF-induced mRNA expression levels of *PXR*.

CYP3A4*1G affects CYP3A4 and CYP3A5 activity in HepG2 Cells

In order to further study the effects of *CYP3A4*1G* on enzyme activity of CYP3A4 and CYP3A5, CYP3A4 enzyme activity and tacrolimus metabolism were also evaluated. CYP3A4 enzyme activity decreased in *CYP3A4*1G* AA, and GA HepG2 cells compared with *CYP3A4*1G* GG HepG2 cells, and CYP3A4 enzyme activity in *CYP3A4*1G* GA HepG2 cells was the lowest of the three (both $P < 0.01$) (Fig.6A). Similarly, for CYP3A5 metabolism, the amount of tacrolimus metabolized

in *CYP3A4*1G* GA HepG2 cells was lower than those in *CYP3A4*1G* GG ($P < 0.01$) and AA HepG2 cells ($P < 0.05$), while there was no significant difference between *CYP3A4*1G* AA and GG HepG2 cells (Fig.6B).

Discussion

CYP3A plays a critical role in the metabolism of drugs and other exogenous and endogenous substances, and its function is modified by genetic factors (Zhai *et al*., 2022). *CYP3A4*1G* affects drug metabolisms by altering *CYP3A4* expression and enzyme activity *in vivo* and in human liver tissues (Miura *et al*., 2011; He *et al*., 2014; Yuan *et al*., 2015). Our previous study showed *CYP3A4*1G* as an enhancer, regulating *CYP3A4* expression indirectly in an allele-dependent manner (Yang *et al*., 2015). Until now, due mainly to the lack of validated *CYP3A4*1G* cell models, it was not clear whether the *CYP3A4*1G* variant could regulate *CYP3A4* expression and metabolism in gene-edited cells. Therefore, in this study we constructed the homozygous point mutations, *CYP3A4*1G* GG, and AA in HepG2 cells using CRISPR/Cas9. These *CYP3A4*1G* HepG2 cells may provide cell models for studying the molecular mechanism by which *CYP3A4*1G* regulates *CYP3A4* and *CYP3A5* expression, and through further CRISPR/Cas9 induced SNPs, provide a means to research the mechanisms of *CYP3A5*3*, or its linkage with *CYP3A4*1G*, in regulating *CYP3A5*.

Our results showed that *CYP3A4*1G* regulates basal expression of *CYP3A4* mRNA and protein, in an allele-dependent manner (Fig.4A, 4B), and that *CYP3A4* expression in *CYP3A4*1G* AA HepG2 cells is lower than that in *CYP3A4*1G* GG HepG2 cells. These findings further support our previous, *in vitro*, luciferase enhancer reporter assays, that showed the *CYP3A4*1G* A allele has a lower enhancer activity than *CYP3A4*1G* G allele in a reverse orientation (Yang *et al*., 2015). Moreover, the

results are consistent with studies in liver microsomes (Yuan *et al*., 2015) and pharmacokinetic studies among *CYP3A5* expressers (Miura *et al*., 2011; Liu *et al*., 2017). For example, Miura *et al*. suggested that *CYP3A4*1G* A allele carriers are related to the lower dose-adjusted area under the concentration-time curve (0-12) of tacrolimus than those with *CYP3A4*1G* GG genotype among *CYP3A5* expressers, but not *CYP3A5* non-expressers (Miura *et al*., 2011). Moreover, among *CYP3A5* non-expressers, He *et al*. also showed *CYP3A4*1G* AA and GA groups have lower area under the concentration-time curve (0-∞) versus the *CYP3A4*1G GG* group (He *et al*., 2014). Importantly, to better understand the molecular mechanism of the *CYP3A4*1G* enhancer's regulation of *CYP3A4* through transcription factor binding, studies using these *CYP3A4*1G* HepG2 cell models should be conducted in the future.

Similar to *CYP3A4*, *CYP3A4*1G* also regulates basal expression of *CYP3A5* in different *CYP3A4*1G* genotype HepG2 cells (Fig.4C, 4D). It may be because of the strong linkage relation between the *CYP3A5*3* G variant allele and *CYP3A4*1G* G wildtype allele as well as *CYP3A5*3* A wildtype allele and *CYP3A4*1G* A variant allele (Uesugi *et al*., 2013; Qi *et al*., 2022). We believe the lower *CYP3A5* expression shown by *CYP3A4*1G* AA HepG2 cells, compared to the *CYP3A4*1G* GG and GA HepG2 cells, is a result of the *CYP3A5*3* G allele forming a new linkage with the *CYP3A4*1G* A allele, which replaces primary G wildtype allele, and *CYP3A4*1G* A allele having lower enhancer activity than the *CYP3A4*1G* G allele. Conversely, in *CYP3A4*1G* GG HepG2 cells, as the *CYP3A5*3* A wildtype allele forms a new

linkage with the *CYP3A4*1G* G wildtype allele (which replaces the primary A variant allele), and *CYP3A4*1G* G allele having a higher enhancer activity than *CYP3A4*1G* A allele, results in *CYP3A4*1G* GG HepG2 cells having higher *CYP3A5* expression than the other *CYP3A4*1G* genotype HepG2 cells. Similar to our study, Dorr *et al*., used CRISPR/Cas9 to confirm the *CYP3A5*3* A allele increased *CYP3A5* expression, furthering the metabolism of midazolam and tacrolimus by editing *CYP3A5*3 GG* into AA and AG genotype in Huh7 cells carrying *CYP3A4*1G* GA and *CYP3A4*22* CC genotypes (Dorr *et al*., 2017). Another study revealed that *CYP3A4*1G* A allele acts as a marker for *CYP3A5*3* A allele, which increases tacrolimus clearance in Japanese liver transplant patients (Uesugi *et al*., 2013); also supporting the regulatory relationship of *CYP3A4*1G* and *CYP3A5*3* in our present study.

Accordingly, through CYP3A4 and CYP3A5 metabolic functional studies, we also found *CYP3A4*1G* decreases CYP3A4 enzyme activity and tacrolimus metabolism in *CYP3A4*1G* GA HepG2 cells. This finding similar to previous results that dose-adjusted C_0 in *CYP3A4*1G* carriers is lower than *CYP3A4*1G* GG individuals in *CYP3A5* expressers (Miura *et al*., 2011). Enzyme activity may be affected by post-transcriptional regulation (protein expression) or post-translational modifications (phosphorylation, etc.). *CYP3A4*1G* affecting CYP3A4 enzyme is partly different from its role for *CYP3A4* expression; it is suspected that multisite phosphorylation of CYP3A4 is associated with enhancing its gp78- and CHIP-mediated ubiquitination (Wang *et al*., 2012; Kwon *et al*., 2019).

Taken together, our results show that *CYP3A4*1G* regulates basal expression and

enzyme activity of *CYP3A4* and *CYP3A5* in different *CYP3A4*1G* genotype HepG2 cells with the *CYP3A5*3* AG genotype. Lin *et al.* found that, in people with the *CYP3A5*3* AG genotype, there is a certain correlation between *CYP3A4* and *CYP3A5* protein and mRNA, and speculated there may be conserved 5′-flanking region elements involved in constitutive expression of *CYP3A4* and *CYP3A5* through sharing a common regulatory pathway (Lin *et al*., 2002). In agreeance with this, in HepG2 cells with *CYP3A5*3* AG genotype, we found that *CYP3A4*1G*, as an enhancer, regulates expression of *CYP3A4* and *CYP3A5*. In addition, Collins and Wang proposed that *CYP3A4*1G* down-regulates *CYP3A4* and *CYP3A5* expression through a lncRNA, AC069294.1 (Collins and Wang, 2022). Further validation will be done in these various *CYP3A4*1G* different HepG2 cells. *CYP3A4*1G* decreases CYP3A4 enzyme activity and tacrolimus metabolism in *CYP3A4*1G* GA HepG2 cells, revealing that individuals with *CYP3A5*3* AG and *CYP3A4*1G* GA genotype, requires a lower dose of tacrolimus than those with *CYP3A5*3* AG and *CYP3A4*1G* GG or AA genotype.

We also found that *CYP3A4*1G* regulates the RIF-induced expression of *CYP3A4* and *CYP3A5* in a *CYP3A4*1G* allele-dependent manner in HepG2 cells (Fig. 5A, 5B). It is well known that RIF increases expression of *CYP3A4* by regulating the transcription factor PXR. Meanwhile, we found that *CYP3A4*1G* may also affect *PXR* expression. Therefore, we believe that *CYP3A4*1G* and RIF act together on PXR to regulate *CYP3A4* and *CYP3A5* expression. As to the relation of *CYP3A5* expression and RIF, our results are consistent with Burk group's suggestion that in

liver tissue, RIF-induced *CYP3A5* expression may phenocopy the effects of the *CYP3A5*3* A, high expression allele (Burk *et al*., 2004). Barwick *et al*. and Burk *et al*. found that RIF inductions of *CYP3A4* and *CYP3A5* share a similar mechanism in which the induction is mediated by the proximal everted repeat sequence separated by 6 bp (ER6) binding site for PXR in the promoter of *CYP3A4* or *CYP3A5* (Barwick *et al*., 1996; Burk *et al*., 2004). This still leads to two speculations. In combination with RIF, *CYP3A4*1G* enhances expression of *CYP3A4* or *CYP3A5* by PXR and its ER6 regulatory element in the *CYP3A4* or *CYP3A5* proximal 5′promoter. Furthermore, *CYP3A4*1G* alone can also enhance expression of *CYP3A4* or *CYP3A5* through PXR and its ER6 regulatory element in *CYP3A4* or *CYP3A5* proximal 5′promoter. Thus, further studies using *CYP3A4*1G* HepG2 cells, with or without RIF, are required to elucidate the molecular mechanisms by which *CYP3A4*1G*, as an enhancer, regulates *CYP3A4* or *CYP3A5* expression through PXR binding the ER6 regulatory element in the *CYP3A4* or *CYP3A5* proximal 5′promoter.

There are some limitations in this study. There is no data showing how *CYP3A4*1G* GG, GA, and AA genotypes affect the actual drug metabolism of CYP3A4 substrates. Furthermore, similar to other CRISPR/Cas9 edited cells, in these point mutation *CYP3A4*1G* GG and AA HepG2 cells, there are also a few bases deletions in *CYP3A4* intron 10 near *CYP3A4*1G* site. There are also a few base substitutions/insertions and deletions of 14 bases near the location of off-targets on chr7 of *CYP3A7* gene far away from *CYP3A4*, although they have no obvious effects on the *CYP3A4*1G* regulated *CYP3A4* and *CYP3A5* expression, or combination with

RIF treatment, in the present study.

In conclusion, we constructed *CYP3A4*1G* GG and AA point mutation HepG2 cell strains, and found *CYP3A4*1G* regulating both basal and RIF-induced expression and enzyme activity of *CYP3A4* and *CYP3A5*. These findings will provide a new theoretical basis for clinical precision therapy based on *CYP3A4*1G* as a biomarker. Considering the linkage relation of *CYP3A4*1G* and *CYP3A5*3*, and complex of CYP3A substrates, use of *CYP3A4*1G*, *CYP3A5*3* and *CYP3A4*22* as biomarkers is recommended to guide CYP3A precision therapy.

Authorship Contributions

Participated in research design: Yang, L.R. Zhang, Zhao and Z. Zhang.

Conducted experiments: Yang, Zhao, Dou, Chang and Xu.

Performed data analysis: Yang, Zhao, Dou and Xu.

Wrote or contributed to the writing of the manuscript: Yang, Zhao, L.R. Zhang, P. Wang, Qiao, Chang and X.F. Wang.

Reference

Barwick JL, Quattrochi LC, Mills AS, Potenza C, Tukey RH, and Guzelian PS (1996) Trans-species gene transfer for analysis of glucocorticoid-inducible transcriptional activation of transiently expressed human CYP3A4 and rabbit CYP3A6 in primary cultures of adult rat and rabbit hepatocytes. *Molecular pharmacology* **50**:10-16.

Bu Y and Gelman IH (2007) v-Src-mediated down-regulation of SSeCKS metastasis suppressor gene promoter by the recruitment of HDAC1 into a USF1-Sp1-Sp3 complex. *The Journal of biological chemistry* **282**:26725-26739.

Burk O, Koch I, Raucy J, Hustert E, Eichelbaum M, Brockmöller J, Zanger UM, and Wojnowski L (2004) The induction of cytochrome P450 3A5 (CYP3A5) in the human liver and intestine is mediated by the xenobiotic sensors pregnane X receptor (PXR) and constitutively activated receptor (CAR). *The Journal of biological chemistry* **279**:38379-38385.

Collins JM and Wang D (2022) Regulation of CYP3A4 and CYP3A5 by a lncRNA: a potential underlying mechanism explaining the association between CYP3A4*1G and CYP3A metabolism. *Pharmacogenetics and genomics* **32**:16-23.

Dong ZL, Li H, Chen QX, Hu Y, Wu SJ, Tang LY, Gong WY, Xie GH, and Fang XM (2012) Effect of CYP3A4*1G on the fentanyl consumption for intravenous patient-controlled analgesia after total abdominal hysterectomy in Chinese Han population. *Journal of clinical pharmacy and therapeutics* **37**:153-156.

Dorr CR, Remmel RP, Muthusamy A, Fisher J, Moriarity BS, Yasuda K, Wu B, Guan W, Schuetz EG, Oetting WS, Jacobson PA, and Israni AK (2017) CRISPR/Cas9

Genetic Modification of CYP3A5 *3 in HuH-7 Human Hepatocyte Cell Line Leads to Cell Lines with Increased Midazolam and Tacrolimus Metabolism. *Drug metabolism and disposition* **45**:957-965.

Gao Y, Zhang LR, and Fu Q (2008) CYP3A4*1G polymorphism is associated with lipid-lowering efficacy of atorvastatin but not of simvastatin. *European journal of clinical pharmacology* **64**:877-882.

He BX, Shi L, Qiu J, Tao L, Li R, Yang L, and Zhao SJ (2011) A functional polymorphism in the CYP3A4 gene is associated with increased risk of coronary heart disease in the Chinese Han population. *Basic & clinical pharmacology & toxicology* **108**:208-213.

He BX, Shi L, Qiu J, Zeng XH, and Zhao SJ (2014) The effect of CYP3A4*1G allele on the pharmacokinetics of atorvastatin in Chinese Han patients with coronary heart disease. *Journal of clinical pharmacology* **54**:462-467.

Hegde N, Joshi S, Soni N, and Kushalappa AC (2021) The caffeoyl-CoA O-methyltransferase gene SNP replacement in Russet Burbank potato variety enhances late blight resistance through cell wall reinforcement. *Plant cell reports* **40**:237-254.

Kato M, Zhang J, Wang M, Lanting L, Yuan H, Rossi JJ, and Natarajan R (2007) MicroRNA-192 in diabetic kidney glomeruli and its function in TGF-beta-induced collagen expression via inhibition of E-box repressors. *Proceedings of the National Academy of Sciences of the United States of America* **104**:3432-3437.

Kuehl P, Zhang J, Lin Y, Lamba J, Assem M, Schuetz J, Watkins PB, Daly A,

Wrighton SA, Hall SD, Maurel P, Relling M, Brimer C, Yasuda K, Venkataramanan R, Strom S, Thummel K, Boguski MS, and Schuetz E (2001) Sequence diversity in CYP3A promoters and characterization of the genetic basis of polymorphic CYP3A5 expression. *Nature genetics* **27**:383-391.

Kwon D, Kim SM, Jacob P, Liu Y, 3rd, and Correia MA (2019) Induction via Functional Protein Stabilization of Hepatic Cytochromes P450 upon gp78/Autocrine Motility Factor Receptor (AMFR) Ubiquitin E3-Ligase Genetic Ablation in Mice: Therapeutic and Toxicological Relevance. *Molecular pharmacology* **96**:641-654.

Lin YS, Dowling AL, Quigley SD, Farin FM, Zhang J, Lamba J, Schuetz EG, and Thummel KE (2002) Co-regulation of CYP3A4 and CYP3A5 and contribution to hepatic and intestinal midazolam metabolism. *Molecular pharmacology* **62**:162-172.

Liu MZ, He HY, Zhang YL, Hu YF, He FZ, Luo JQ, Luo ZY, Chen XP, Liu ZQ, Zhou HH, Shao MJ, Ming YZ, Xin HW, and Zhang W (2017) IL-3 and CTLA4 gene polymorphisms may influence the tacrolimus dose requirement in Chinese kidney transplant recipients. *Acta pharmacologica Sinica* **38**:415-423.

Liu H, Jing Y, Zou D, Hou X, Peng H, Zhou J, Li Y, Xiong D, Wen J, and Wei X (2020) Regulation of indirubin derivative PHⅡ-7 on tacrolimus transport and metabolism via PXR-CYP3 A5 /ABCB1 signaling pathway and its mechanism. *Chinese Pharmacological Bulletin* **36**:927-934.

López-Terrada D, Cheung SW, Finegold MJ, and Knowles BB (2009) Hep G2 is a

hepatoblastoma-derived cell line. *Human pathology* **40**:1512-1515.

Lv J, Liu F, Feng N, Sun X, Tang J, Xie L, and Wang Y (2018) CYP3A4 gene polymorphism is correlated with individual consumption of sufentanil. *Acta anaesthesiologica Scandinavica* **62**:1367-1373.

Miura M, Satoh S, Kagaya H, Saito M, Numakura K, Tsuchiya N, and Habuchi T (2011) Impact of the CYP3A4*1G polymorphism and its combination with CYP3A5 genotypes on tacrolimus pharmacokinetics in renal transplant patients. *Pharmacogenomics* **12**:977-984.

Mulder TAM, van Eerden RAG, de With M, Elens L, Hesselink DA, Matic M, Bins S, Mathijssen RHJ, and van Schaik RHN (2021) CYP3A4*22 Genotyping in Clinical Practice: Ready for Implementation? *Frontiers in genetics* **12**:711943.

Pande P, Zhong XB, and Ku WW (2020) Histone Methyltransferase G9a Regulates Expression of Nuclear Receptors and Cytochrome P450 Enzymes in HepaRG Cells at Basal Level and in Fatty Acid Induced Steatosis. *Drug metabolism and disposition* **48**:1321-1329.

Qi G, Han C, Zhou Y, and Wang X (2022) Allele and genotype frequencies of CYP3A4, CYP3A5, CYP3A7, and GSTP1 gene polymorphisms among mainland Tibetan, Mongolian, Uyghur, and Han Chinese populations. *Clinical and experimental pharmacology & physiology* **49**:219-227.

Ren ZY, Xu XQ, Bao YP, He J, Shi L, Deng JH, Gao XJ, Tang HL, Wang YM, and Lu L (2015) The impact of genetic variation on sensitivity to opioid analgesics in patients with postoperative pain: a systematic review and meta-analysis. *Pain*

physician **18**:131-152.

Shi C, Yan L, Gao J, Chen S, and Zhang L (2022) Effects of ABCB1 DNA methylation in donors on tacrolimus blood concentrations in recipients following liver transplantation. *British journal of clinical pharmacology* **88**:4505-4514.

Tang J, Xu J, Zhang YL, Liu R, Liu MZ, Hu YF, Shao MJ, Zhu LJ, Cao S, Xin HW, Feng GW, Shang WJ, Meng XG, Zhang LR, Ming YZ, Zhang W, and Zhou G (2019) Incorporation of Gene-Environment Interaction Terms Improved the Predictive Accuracy of Tacrolimus Stable Dose Algorithms in Chinese Adult Renal Transplant Recipients. *Journal of clinical pharmacology* **59**:890-899.

Uesugi M, Hosokawa M, Shinke H, Hashimoto E, Takahashi T, Kawai T, Matsubara K, Ogawa K, Fujimoto Y, Okamoto S, Kaido T, Uemoto S, and Masuda S (2013) Influence of cytochrome P450 (CYP) 3A4*1G polymorphism on the pharmacokinetics of tacrolimus, probability of acute cellular rejection, and mRNA expression level of CYP3A5 rather than CYP3A4 in living-donor liver transplant patients. *Biological & pharmaceutical bulletin* **36**:1814-1821.

Wang D, Chen H, Momary KM, Cavallari LH, Johnson JA, and Sadée W (2008) Regulatory polymorphism in vitamin K epoxide reductase complex subunit 1 (VKORC1) affects gene expression and warfarin dose requirement. *Blood* **112**:1013-1021.

Wang D, Guo Y, Wrighton SA, Cooke GE, and Sadee W (2011) Intronic polymorphism in CYP3A4 affects hepatic expression and response to statin drugs. *The pharmacogenomics journal* **11**:274-286.

Wang D and Sadee W (2016) CYP3A4 intronic SNP rs35599367 (CYP3A4*22) alters RNA splicing. *Pharmacogenetics and genomics* **26**:40-43.

Wang Y, Guan S, Acharya P, Liu Y, Thirumaran RK, Brandman R, Schuetz EG, Burlingame AL, and Correia MA (2012) Multisite phosphorylation of human liver cytochrome P450 3A4 enhances Its gp78- and CHIP-mediated ubiquitination: a pivotal role of its Ser-478 residue in the gp78-catalyzed reaction. *Molecular & cellular proteomics* **11**:M111.010132.

Yang W, Zhao D, Han S, Tian Z, Yan L, Zhao G, Kan Q, Zhang W, and Zhang L (2015) CYP3A4*1G regulates CYP3A4 intron 10 enhancer and promoter activity in an allelic-dependent manner. *International journal of clinical pharmacology and therapeutics* **53**:647-657.

Yuan JJ, Hou JK, Zhang W, Chang YZ, Li ZS, Wang ZY, Du YY, Ma XJ, Zhang LR, Kan QC, and Candiotti KA (2015) CYP3A4*1G Genetic Polymorphism Influences Metabolism of Fentanyl in Human Liver Microsomes in Chinese Patients. *Pharmacology* **96**:55-60.

Yuan R, Zhang X, Deng Q, Wu Y, and Xiang G (2011) Impact of CYP3A4*1G polymorphism on metabolism of fentanyl in Chinese patients undergoing lower abdominal surgery. *Clinica chimica acta* **412**:755-760.

Zhai Q, van der Lee M, van Gelder T, and Swen JJ (2022) Why We Need to Take a Closer Look at Genetic Contributions to CYP3A Activity. *Frontiers in pharmacology* **13**:912618.

Zhang H, Chen M, Wang X, and Yu S (2017) Patients with CYP3A4*1G genetic

polymorphism consumed significantly lower amount of sufentanil in general anesthesia during lung resection. *Medicine* **96**: e6013.

Zhang J, Zhang L, Zhao X, Shen S, Luo X, and Zhang Y (2018) Association between MDR_1/CYP3A4/$OPRM_1$ gene polymorphisms and the post-caesarean fentanyl analgesic effect on Chinese women. *Gene* **661**:78-84.

Zhang W, Chang YZ, Kan QC, Zhang LR, Li ZS, Lu H, Wang ZY, Chu QJ, and Zhang J (2010) CYP3A4*1G genetic polymorphism influences CYP3A activity and response to fentanyl in Chinese gynecologic patients. *European journal of clinical pharmacology* **66**:61-66.

Zhao YL YW, Zhang LR (2016) Genotype analysis of CYP3A, SLCO1B1 and POR in HepG2 cells. *Journal of Zhengzhou University (Medical Sciences)* **51**:583-587.

Acknowledgements

This work was supported by the National Natural Science Foundation of the People's Republic of China [grant number 81773815] and by the Project of Science and Technology Department of Henan Province of China [grant number 222102310186 and 162102310523].

Conflicts of Interest

No author has an actual or perceived conflict of interest with the contents of this article.

Figure legends:

Fig.1 The location of *CYP3A4*1G*, *CYP3A5*3* and their linkage disequilibrium relation

Rs2242480 and rs776746 indicate *CYP3A4*1G* and *CYP3A5*3*, respectively.

Fig.2 *CYP3A4*1G* allele (rs2242480) and guide RNA targeting strategy

Guide RNAs were targeted to protospacer adjacent motif (PAM) sequences on same side of the *CYP3A4*1G* allele (sg-2W and sg-3M locus). *CYP3A4* exon 10 sequence is in capital letters, and the downstream intron 10 sequence is in lower-case letters.

Fig.3 Sequencing results of gene-edited *CYP3A4*1G* HepG2 cells

GA, GG, and AA indicate sequencing results of *CYP3A4*1G* GA, GG, and AA HepG2 cells, respectively. *CYP3A4*1G* GA HepG2 cells are the control. A base with a red circle in the sequence shows the *CYP3A4*1G* site and corresponding genotype.

Fig.4 *CYP3A* basal expression in *CYP3A4*1G* GG, GA, and AA HepG2 cells

CYP3A4 mRNA (A) and protein (B) expression levels in *CYP3A4*1G* GG, GA, and AA HepG2 cells. *CYP3A5* mRNA (C) and protein (D) expression levels in *CYP3A4*1G* GG, GA, and AA HepG2 cells. The error bars represent S.D. (n=3 per group for mRNA and protein). (**P* < 0.05, ***P* < 0.01)

Fig.5 *CYP3A* induction expression by RIF in *CYP3A4*1G* GG, GA, and AA HepG2 cells

CYP3A (A, B) and *PXR* (C) mRNA expression in *CYP3A4*1G* GG, GA, and AA HepG2 cells after 48 h induced by rifampicin (RIF). DMSO group for control. The error bars represent S.D. (n=3 per group for mRNA). (**P* < 0.05, ***P* < 0.01 vs. GG

or GA control group; $^{\#}P < 0.05$, $^{\#\#}P < 0.01$ vs. the same genotype control group; $^{\wedge}P < 0.05$, $^{\wedge\wedge}P < 0.01$ vs. GG or GA RIF group)

Fig.6 CYP3A4 enzyme activity and tacrolimus metabolism study in *CYP3A4*1G* GG, GA, and AA HepG2 cells

CYP3A4 enzyme activity levels (A) and tacrolimus metabolism study (B) in *CYP3A4*1G* GG, GA, and AA HepG2 cells. The amount of tacrolimus metabolized in *CYP3A4*1G* GG, GA, and AA HepG2 cells is shown. (n=3 per group for CYP3A4 enzyme activity and tacrolimus metabolism). The error bars represent S.D. ($^{*}P < 0.05$, $^{**}P < 0.01$)

DMD Fast Forward. Published on January 9, 2023 as DOI: 10.1124/dmd.122.001111
This article has not been copyedited and formatted. The final version may differ from this version.

Fig.1

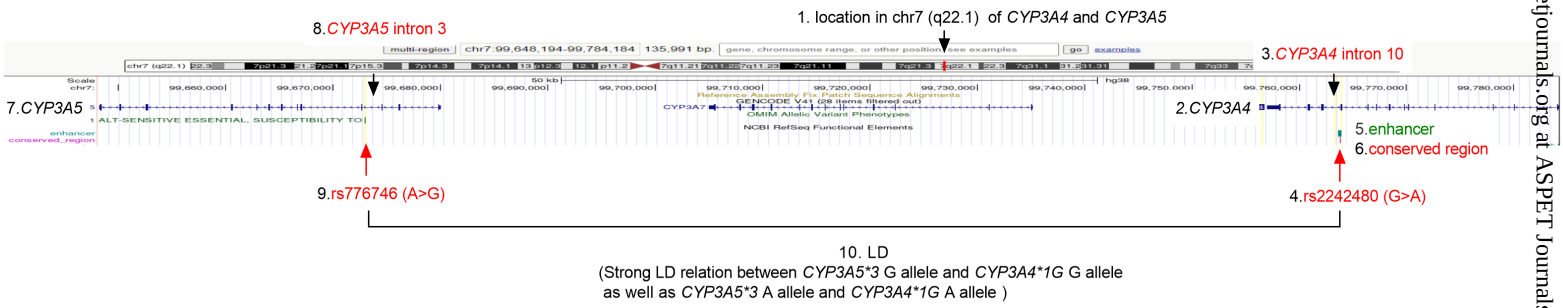

DMD Fast Forward. Published on January 9, 2023 as DOI: 10.1124/dmd.122.001111
This article has not been copyedited and formatted. The final version may differ from this version.

Fig.2

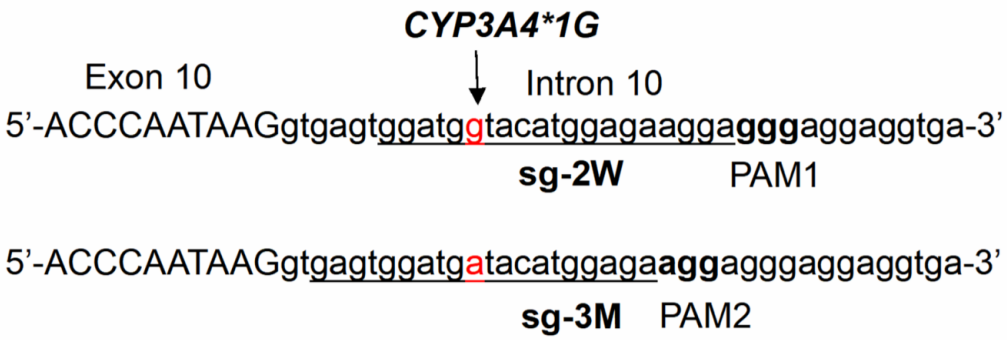

DMD Fast Forward. Published on January 9, 2023 as DOI: 10.1124/dmd.122.001111
This article has not been copyedited and formatted. The final version may differ from this version.

Fig.3

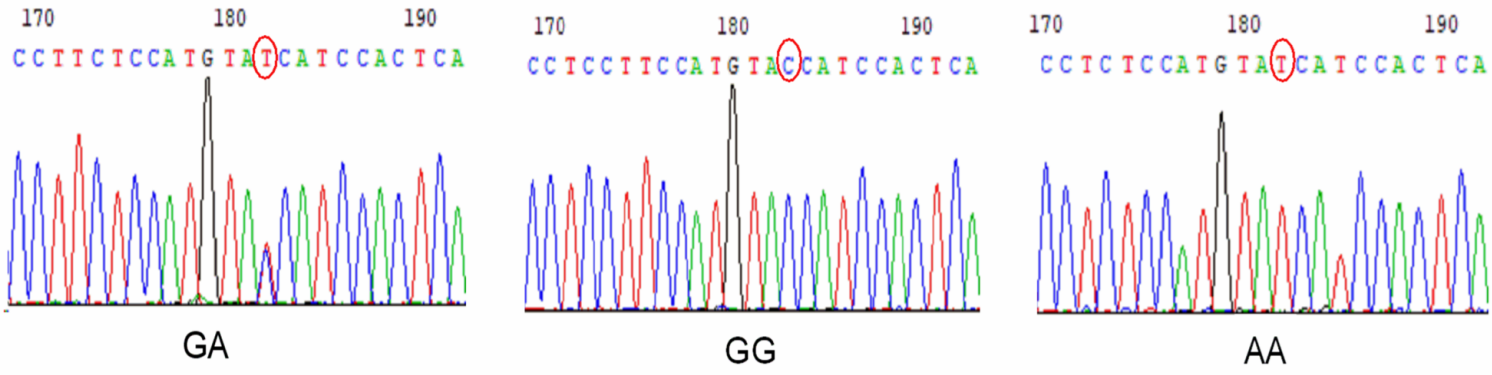

DMD Fast Forward. Published on January 9, 2023 as DOI: 10.1124/dmd.122.001111
This article has not been copyedited and formatted. The final version may differ from this version.

Fig.4

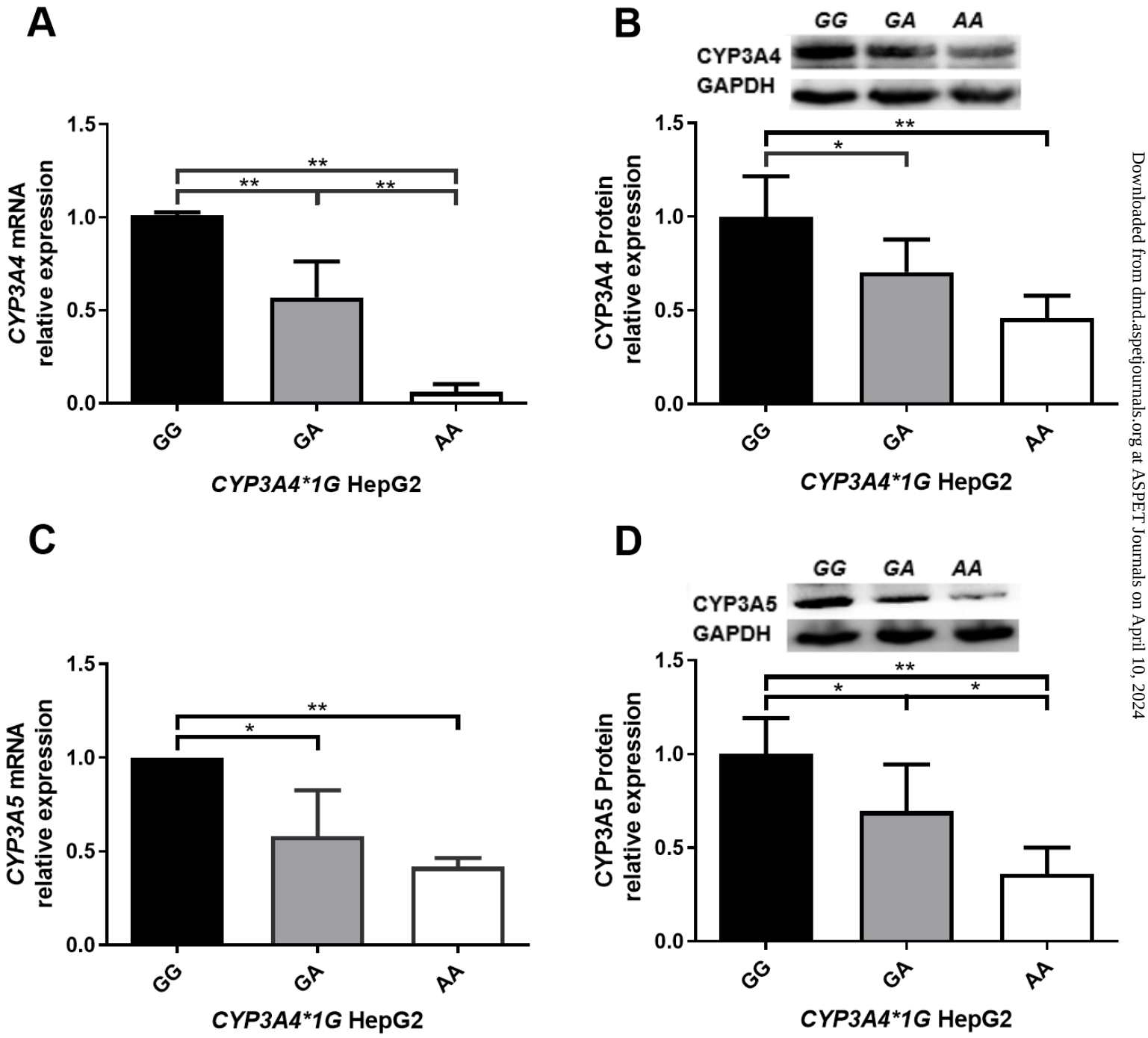

DMD Fast Forward. Published on January 9, 2023 as DOI: 10.1124/dmd.122.001111
This article has not been copyedited and formatted. The final version may differ from this version.

Fig.5

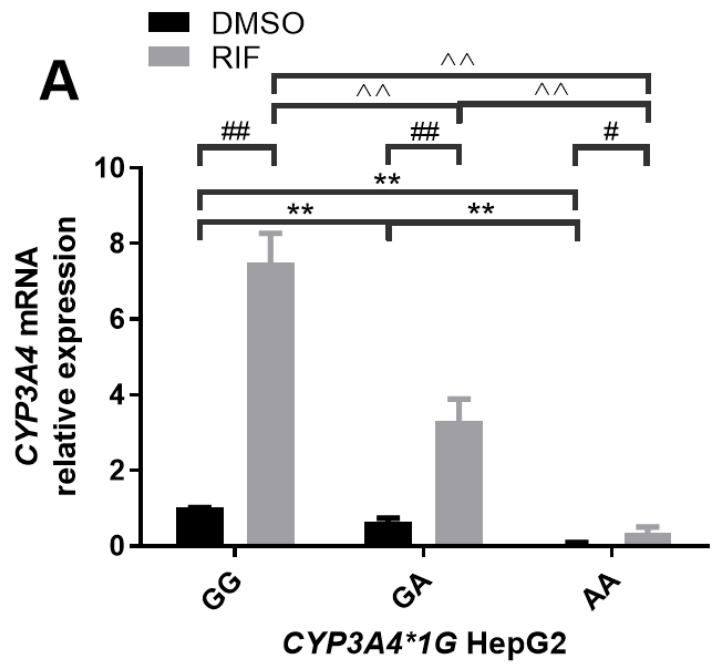

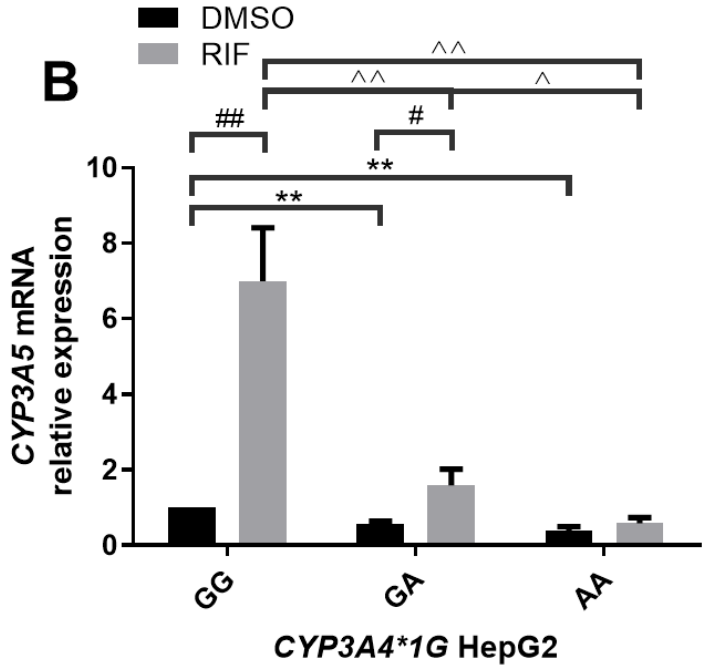

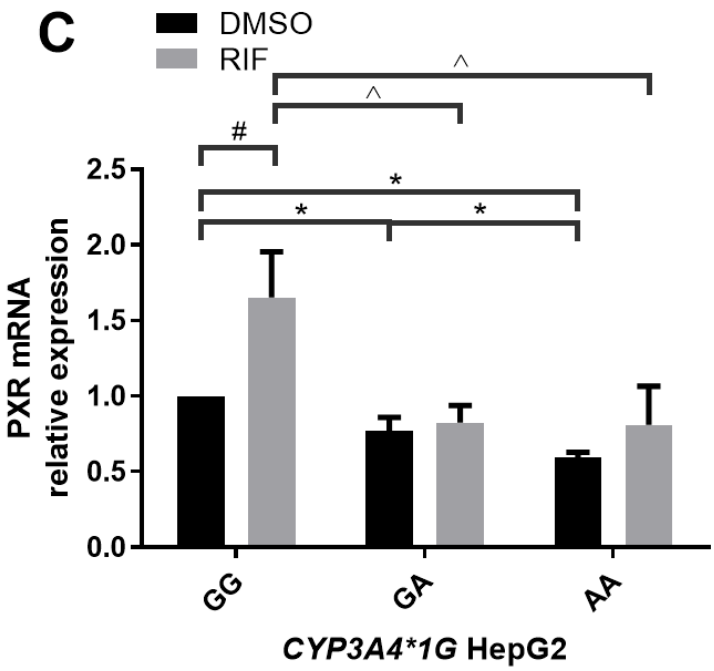

DMD Fast Forward. Published on January 9, 2023 as DOI: 10.1124/dmd.122.001111
This article has not been copyedited and formatted. The final version may differ from this version.

Fig.6